



Research article

Influence of a pro-inflammatory stimulus on the miRNA and lipid content of human dental stem cell-derived extracellular vesicles and their impact on microglial activation

Viridiane Gratpain^a, Axelle Lorient^b, Pauline Bottemanne^c, Ludovic d'Auria^d, Romano Terrasi^c, Valéry L. Payen^a, Vincent van Pesch^d, Giulio G. Muccioli^c, Anne des Rieux^{a,*}

^a Louvain Drug Research Institute, Advanced Drug Delivery and Biomaterials, Université Catholique de Louvain, UCLouvain, 1200, Brussels, Belgium

^b de Duve Institute, Computational Biology Unit, Université Catholique de Louvain, UCLouvain, 1200, Brussels, Belgium

^c Louvain Drug Research Institute, Bioanalysis and Pharmacology of Bioactive Lipids, Université Catholique de Louvain, UCLouvain, 1200, Brussels, Belgium

^d Institute of Neuroscience, Neurochemistry Unit, Université Catholique de Louvain, UCLouvain, 1200, Brussels, Belgium

ARTICLE INFO

Keywords:

Extracellular vesicles
Mesenchymal stem cells
Size-exclusion chromatography
Neuroinflammation
miRNA
Lipidomics

ABSTRACT

Neuro-inflammation occurs in numerous disorders such as multiple sclerosis, Alzheimer's disease and Parkinson's disease. However, anti-inflammatory drugs for the central nervous system have failed to show significant improvement when compared to a placebo in clinical trials. Our previous work demonstrated that stem cells from the apical papilla (SCAP) can decrease neuro-inflammation and stimulate oligodendrocyte progenitor cell differentiation. One hypothesis is that the therapeutic effect of SCAP could be mediated by their secretome, including extracellular vesicles (EV). Here, our objectives were to characterize SCAP-EV and to study their effect on microglial cells. We isolated EV from non-activated SCAP and from SCAP activated with TNF α and IFN- γ and characterized them according to their size, EV markers, miRNA and lipid content. Their ability to decrease pro-inflammatory cytokine expression *in vitro* and *ex vivo* was also assessed. We showed that the miRNA content was impacted by a pro-inflammatory environment but not their lipid composition. SCAP-EV reduced the expression of pro-inflammatory markers in LPS-activated microglial cells while their effect was limited on mouse spinal cord sections. In conclusion, we were able to isolate EV from SCAP, to show that their miRNA content was impacted by a pro-inflammatory stimulus, and to describe that SCAP-EV and not the protein fraction of conditioned medium could reduce pro-inflammatory marker expression in LPS-activated BV2 cells.

Abbreviations: EV, extracellular vesicles; SCAP, stem cells from the apical papilla; MSC, mesenchymal stem cell; SEC, size exclusion chromatography; NTA, nanoparticle Tracking Analysis; DELFIA, dissociation-enhanced lanthanide fluorescence immunoassay; TNF α , tumor necrosis factor α ; IFN γ , interferon γ ; miRNA, microRNA; LPS, lipopolysaccharide; IL-6, interleukine-6; IL-1 β , interleukine-1 β ; iNOS, inducible nitric oxide synthase.

* Corresponding author.

E-mail address: anne.desrieux@uclouvain.be (A. des Rieux).

<https://doi.org/10.1016/j.heliyon.2024.e27025>

Received 14 August 2023; Received in revised form 21 February 2024; Accepted 22 February 2024

Available online 2 March 2024

2405-8440/© 2024 Published by Elsevier Ltd. This is an open access article under the CC BY-NC-ND license (<http://creativecommons.org/licenses/by-nc-nd/4.0/>).

1. Introduction

Once it became apparent that extracellular vesicles (EV) were involved in local and systemic cell communication [1,2], extensive studies have been conducted to elucidate their role in pathology development and regulation, making them potential biomarker of various diseases, mostly cancer [3–5]. Furthermore, EV play a crucial role in physiological processes such as immune regulation, leading to the development of therapeutic approaches using these vesicles [6]. Recently, the use of EV as a drug delivery vehicle has also raised a lot of interest. Indeed, EV are nanoscale vesicles that can be loaded with a specific bioactive molecule (i.e. miRNA, lipid, small molecule [7]), can cross biological barriers, including the blood brain barrier, are characterized by low immunogenicity [8] and no toxicity [9], and are able to deliver their cargo into recipient cells [10]. EV can be isolated from diverse sources, such as eukaryotic cell and bacteria conditioned media, biological fluids, and plants. Eukaryotic cell-conditioned medium is the preferred source of EV as nanomedicines, as it offers the possibility to scale-up EV production processes [11], to have a better reproducibility of EV isolation compared to other sources, to modify parent cells in order to load a bioactive molecule into EV but also to modify EV composition by changing cell culture conditions [12].

As mesenchymal stem cell (MSC)-derived EV can present similar therapeutic properties as their parent cells [13], they have become a source of choice to produce EV for therapeutic uses. Indeed, recent studies have shown that, like MSC, EV produced by MSC were able to decrease inflammation in mice [14] but also to reduce neurological impairment in neurodegenerative diseases [8]. Our previous work has shown that stem cells from the apical papilla (SCAP) can exert an anti-inflammatory and neuroprotective effect [15] via their secretome [16], notably when subjected to a pro-inflammatory environment. This could be mediated by soluble factors but also by their EV [17].

To the best of our knowledge, no one ever isolated EV from SCAP based on size differentiation, characterized them according to their miRNA and lipid content, and studied their impact on the secretion of inflammatory markers in activated glial cells. We thus optimized a protocol to obtain EV from SCAP-conditioned medium and we characterized them according to MISEV2018 recommendations [18]. Then, as the secretion of immunomodulatory factors by SCAP increased upon exposure to a pro-inflammatory stimulus, we hypothesized that their EV content could be affected as well. Since EV are known to be one of the major vehicles for miRNA trafficking and as lipids are major components of EV membrane, we focused on those two components. Finally, we evaluated whether SCAP-secreted EV (SCAP-EV), produced in steady state or in a pro-inflammatory environment, would have an immunomodulatory action on glial cells. Thus, the aim of this study was to better understand the impact of a pro-inflammatory environment on EV composition and determine whether SCAP-EV would recapitulate SCAP anti-inflammatory effect on glial cells.

2. Materials and methods

All relevant data have been submitted to the EV-TRACK knowledgebase (EV-TRACK ID: EV220308).

2.1. Cell culture and isolation of EV

Previously characterized human SCAP from healthy tooth were used [19]. SCAP were cultured at 37 °C and 5% CO₂ in minimum essential medium Eagle (MEM, Sigma-Aldrich, St Louis, USA) supplemented with 10% fetal bovine serum (FBS), 1% L-glutamine 200 mM (Thermo Fisher Scientific, Waltham, USA), 100 U/mL penicillin and 100 µg/ml streptomycin (Thermo Fisher Scientific). Non-activated and activated SCAP were cultured for 3 days in serum-free MEM and in serum-free MEM containing TNF α (20 ng/ml) and IFN- γ (20 ng/ml), respectively [16]. Conditioned media were then collected and EV were isolated by centrifugation and ultrafiltration followed by size exclusion chromatography (SEC) (Fig. 1A). Briefly cells, dead cells and cell debris were removed by successive centrifugations (300 g for 10 min, 1000 g for 20 min and 10,000 g for 30 min, respectively). The supernatant was then filtrated on 0.22 µm filter and concentrated 200–400 times using an ultrafiltration device with a 30 kDa or a 100 kDa cut-off (Centricon® Plus-70, Merck Millipore, Burlington, USA) until a volume lower than 500 µl was obtained. Finally, small EV (exosomes and small microvesicles) were separated from contaminating proteins using a SEC column (qEV Original® 35 nm or 70 nm, Izon Science, Lyon, France). Fractions from 1 to 30 (500 µl each) were collected. Endotoxin detection and quantification were performed with ToxinSensor™ Chromogenic LAL Endotoxin Assay Kit (GenScript, Piscataway, USA), according to the manufacturer's instructions.

2.2. EV characterization

2.2.1. Protein quantification

Proteins in fractions 1 to 30 were quantified using a Pierce™ bicinchoninic acid (BCA) Protein Assay Kit (Thermo Fisher Scientific).

2.2.2. Nanoparticle tracking analysis (NTA)

Particle concentration was quantified using a ZetaView in all fractions [1–30] (Particle Metrix, Inning am Ammersee, Germany) with a recording video frame set at 60 s. EV were diluted (1:1000–1:2000) in ultrapure water to a concentration ranging between 10⁷–10⁸ particles/mL. Sensitivity was set to 79 and camera shutter to 100. Measurements were averaged from particles counted in 11 different positions for 2 repeated cycles with camera at medium resolution modes. Size distribution and zeta potential were also measured by NTA.

2.2.3. Dissociation-enhanced lanthanide fluorescence immunoassay (DELFIA®)

Fifty μL of each SEC fraction [1–30] were bound to protein-binding ELISA plate (ELISA Strip Plate, 771,261; Greiner Bio-One, Frickenhausen, Germany). After overnight incubation at 4 °C, the plate was shaken on a tilting shaker at 30 rpm at 4 °C. Then the plate was washed 3 times with Delfia buffer (#1244–111; PerkinElmer, Wellesley, USA) diluted to 1x in PBS and blocked for 90 min with 1% BSA in PBS. Primary antibodies against CD9 (MAB1880, R&D Systems, Minneapolis, USA), CD81 (#349502; Biolegend, San Diego, USA), CD63 (MCA2142; Serotec Bio-Rad), Flotillin-1 (#610821; BD Biosciences, San Jose, USA) and ApoB (sc-13538; Santa Cruz) (1 $\mu\text{g}/\text{ml}$ in 1% BSA) were then incubated for 90 min. After 3 washes in the Delfia buffer, goat anti-mouse biotinylated antibody (NEF8232001EA; PerkinElmer) diluted at 0.2 $\mu\text{g}/\text{ml}$ in 0.1% BSA was added for 60 min. After 3 washes, Europium-conjugated Streptavidin (#1244–360; PerkinElmer) diluted at 1:1000 was added for 45 min. After 6 washes, the Delfia enhancement solution (#1244–105; PerkinElmer) was incubated for 15 min. Quantification of the signal was performed using time-resolved fluorometry with excitation/emission 340/615 nm, flash energy/light exposure high/medium and integration lag/counting time 400/400 μs (Victor X4 multilabel plate reader; PerkinElmer).

2.2.4. Western blot

Proteins from 10^9 EV (fractions 7 to 11) and from SCAP were extracted using a RIPA buffer containing EDTA and protease inhibitors. Protein concentration was measured with a Pierce™ BCA Protein Assay Kit (Thermo Fisher Scientific). Lysates were then denatured with Laemmli sample buffer 6x (375 mM Tris-HCl, pH 6.8; 30% glycerol; 9% β -mercaptoethanol; 9% SDS; 0.03% bromophenol blue). Positive (CD81) and negative (Calnexin) markers were analyzed by Western blot after running 12.5 μg of proteins/sample on a sodium dodecyl sulfate–polyacrylamide gel electrophoresis (SDS-PAGE) on a 4–20 % gradient gel (Bio-Rad). Separated proteins were then transferred with a semi-dry method to nitrocellulose membranes (Thermo Fisher Scientific) that were blocked with 5 % dry milk dissolved in Tris-buffered saline. Membranes were then incubated with an *anti*-calnexin antibody (mAb2679, Cell Signaling Technology, Danvers, USA) and an anti-CD81 antibody (sc-166,028, Santa Cruz), diluted at 1:1000. Anti-mouse and anti-rabbit secondary antibodies conjugated to horseradish peroxidase and diluted at 1:10,000 were used for the detection. Membranes were revealed with Pierce™ ECL Western Blotting Substrate (Thermo Fisher Scientific) and images were acquired using Fusion Solo S (Vilber Lourmat, Collégien, France).

2.3. Impact of a pro-inflammatory stimulus on SCAP-EV miRNA content

Total RNA from 5×10^{10} non-activated SCAP-EV and 5×10^{10} activated SCAP-EV was extracted using miRNeasy mini kit (Qiagen) according to the manufacturer's instructions. RNA concentration was measured by Qubit RNA HS assay kit (Q10211, Thermo Fisher Scientific). Small RNA sequencing has been performed using 50 ng of RNA by Genewiz (Azenta Life Sciences, Leipzig, Germany).

Small RNA sequencing data were processed using *mirdeep2* pipeline [20]. Differential expression analysis was done using *DESeq2* v1.32.0 Bioconductor package [21]. miRNA with a p-adjusted value < 0.05 and showing an absolute log-foldchange >1.5 between activated and non-activated samples were considered differentially expressed. *multiMiR* v1.14.0 Bioconductor package [22] was used to predict the miRNA target genes. miRNA-target pairs predicted by at least 3 of the 4 predictions databases interrogated (DIANA-microT, miRDB, PicTar, and TargetScan) were selected. Over-representation analysis were done using *clusterProfiler* 4.0.0 [23] on Kyoto Encyclopedia of Genes and Genomes (KEGG) pathways. Raw data can be found at: <https://www.ncbi.nlm.nih.gov/geo/query/acc.cgi?acc=GSE208577>.

2.4. Influence of SCAP activation on EV lipid content

The lipid content of the different samples was analyzed by Liquid Chromatography coupled to Mass Spectrometry (LC-MS). Briefly, lipids from EV were analyzed after liquid/liquid extraction (CH_2Cl_2 –MeOH– H_2O) in acidic condition in the presence of internal standards (17:0-LPC, 17:1-LPE, 17:1-LPG, 17:1 LPI, 17:0 Sulfatide, 17:0 sphingomyelin, 17:0 Ceramide). A Xevo-TQS (from Waters) coupled to an UPLC was used to analyze the samples with three different methods, according to lipid family.

- For the lysophospholipids, phospholipids, sulfatides and sphingomyelin lipids, an HSS LC-18 column 100×2.1 mm, 1.8 μm (Waters) at a temperature of 40 °C was used. The mobile phase consisted in a gradient between A: MeOH-ACN (9/1, v/v) 75% - H_2O 25%; B: MeOH- ACN (9/1, v/v) and C: IpOH, all containing ammonium acetate (5 mM). An ESI probe operated in negative mode was used for sample ionization.
- For the ceramide, we used a BEH LC-18 column 50×2.1 , 1.7 μm (Waters) at a temperature of 40 °C. The mobile phase consisted in a gradient between A: H_2O 25% - MeOH 75%; B: MeOH 100%, all containing acetic acid (0.1%). An ESI probe operated in negative mode was also used for sample ionization.
- For arachidonic acid derivatives and related compounds, an Acquity UPLC BEH C18 (150×2.1 mm; 1.7 μm) column was used. Mobile phases consisted in H_2O -ACN-acetic acid (94.9:5:0.1; v/v/v) and ACN-acetic acid (99.9:0.1; v/v). An ESI probe operated in negative mode was used for sample ionization.

For all the lipids, the relative quantification was based on the ratio between the area under the curve (AUC) of the lipid of interest and the AUC of the respective internal standard. The data were then normalized to the number of EV in the samples.

2.5. Impact of SCAP-EV on BV2 cell activation

Murine microglial cells (BV2 cells) were cultured at 37 °C and 5% CO₂ in high-glucose DMEM medium with 10% FBS, 100 U/mL penicillin and 100 µg/ml streptomycin. BV2 cells were seeded overnight into 24-well plates (2.5 × 10⁵ cells per well) and incubated for 1 h with fresh culture medium containing 100 ng/ml LPS and 1% EV-depleted FBS (FBS centrifuged for 1 h at 100,000 g to remove EV). LPS concentration was chosen based on previous studies conducted in the lab [24–26]. Then, EV isolated from non-activated or activated SCAP (5 × 10⁹ EV/well) were added to the cells and incubated for 8 h or 24 h before RNA extraction. In a subsequent experiment (same setting: BV2 cells activated with 100 ng/ml of LPS, EV incubated for 8 h before RNA extraction), EV isolated from activated SCAP (Fractions 7–11) were compared to a pool of the protein fractions (Fractions 12–30) obtained from the same sample after SEC.

Total RNA from BV2 cells was extracted using TRIzol™ reagent (Thermo Fisher Scientific) according to the manufacturer's instructions. Reverse transcription was performed using the GoScript Transcription System (Promega, Madison, USA) from 1 µg of total RNA. qPCR was performed with qPCR Master Mix (Promega) and a STEPone PLUS instrument and software (Applied Biosystems, Foster City, USA) as [27]. Data were analyzed with the ΔΔCt method using the 60S ribosomal protein L19 (RPL19) as a reference gene. Primer sequences are given in Table 1.

2.6. Impact of SCAP EV on mouse spinal cord activation

Animal experiments were declared to the ethical committee for animal cares (07-OTLADDB-2023-7). Spinal cord slices were obtained from female C57BL/6J mice. Briefly, the spinal cords were hydro extruded, cut into 400 µm slices in a tissue chopper. The slices (4–5 per well) were incubated in DMEM-F12 media (containing 10 % EV-depleted FBS, 100 U/mL penicillin and 100 µg/ml streptomycin) overnight. They were then stimulated with LPS (100 ng/ml) for 1 h prior to incubation with EV isolated from non-activated or activated SCAP (5 × 10⁹ EV/well) or the vehicle (PBS) for 8 or 24 h. Slices were then recovered and stored at –80 °C until processed for mRNA extraction. Gene expression was analyzed as described in 2.5. TNF-α and IL-6 levels were quantified in the culture medium using respectively Mouse TNF alpha uncoated ELISA kit and Mouse IL-6 uncoated ELISA kit (Invitrogen), according to the manufacturer's instructions.

2.7. Statistical analysis

Statistical analysis was performed using PRISM (GraphPad Software, CA, USA). Error bars represent the standard error of the mean (SEM) in all figures. One-way ANOVA followed by Tukey, or Kruskal-Wallis followed by Dunn's test were performed to compare different conditions (p < 0.05). The number of experiments and the number of replicates are indicated in the figure legends.

3. Results

3.1. Characterization of SCAP-EV

To isolate the EV secreted from SCAP, a combination of 2 methods based on the size of the vesicles was used: ultrafiltration and SEC (Fig. 1A). Two ultrafiltration cut-offs were compared (30 kDa and 100 kDa) as well as two SEC columns (35 nm and 70 nm) to optimize the yield of EV and the elimination of contaminating proteins.

SEC allowed to separate EV from soluble proteins and to obtain EV with a very low soluble protein contamination (Fig. 1B). The pore size of the ultrafiltration units had an impact on the size (Fig. 1C) and on the number of isolated EV per cell (Fig. 1D). Indeed, 2.5 times more vesicles were recovered with units presenting a cut-off of 30 kDa than with units with a cut-off of 100 kDa. No impact of the column type on particle number or size was observed (Fig. 1C & D). For further EV isolations in this work, 30 kDa ultrafiltration units and 35 nm SEC columns have been used.

As the highest concentration of particles was observed in fractions 7 to 11 (Fig. 1B), experiments were performed on a pool of these fractions. The mean size of EV in the pool was 137.5 nm (SD = 49.7 nm).

In order to confirm that the particles in the pool were indeed EV, samples were analyzed by DELFIA® and Western Blotting for positive and negative EV markers (as per MISEV2018 recommendations [18]). Isolated particles from factions 7 to 11 were positive to tetraspanins (CD63, CD81 and CD9) and flotillin (all positive markers of EV) (Fig. 1E & F) while they were negative for calnexin (Fig. 1F) and ApoB (analyzed DELFIA®, no signal), 2 negative markers of EV.

Table 1
List of primers sequences.

Gene	Forward (5'-3')	Reverse (5'-3')
Mouse RPL19	TGACCTGGATGAGAAGGATGAG	CTGTGATACATATGGCGGTCAATC
Mouse IL-6	ACAAGTCGGAGGCTTAATTACACAT	TTGCCATTGCACAACCTCTTTTC
Mouse IL-1β	TCGCTCAGGGTCACAAGAAA	CATCAGAGGCAAGGAGGAAAAC
Mouse iNOS	AGGTACTCAGCGTGCTCCAC	GCACCGAAGATATCTTCATG
Mouse TNFα	AGCCCCAGTCTGTATCCTT	GGTCACTGTCCAGCATCTT

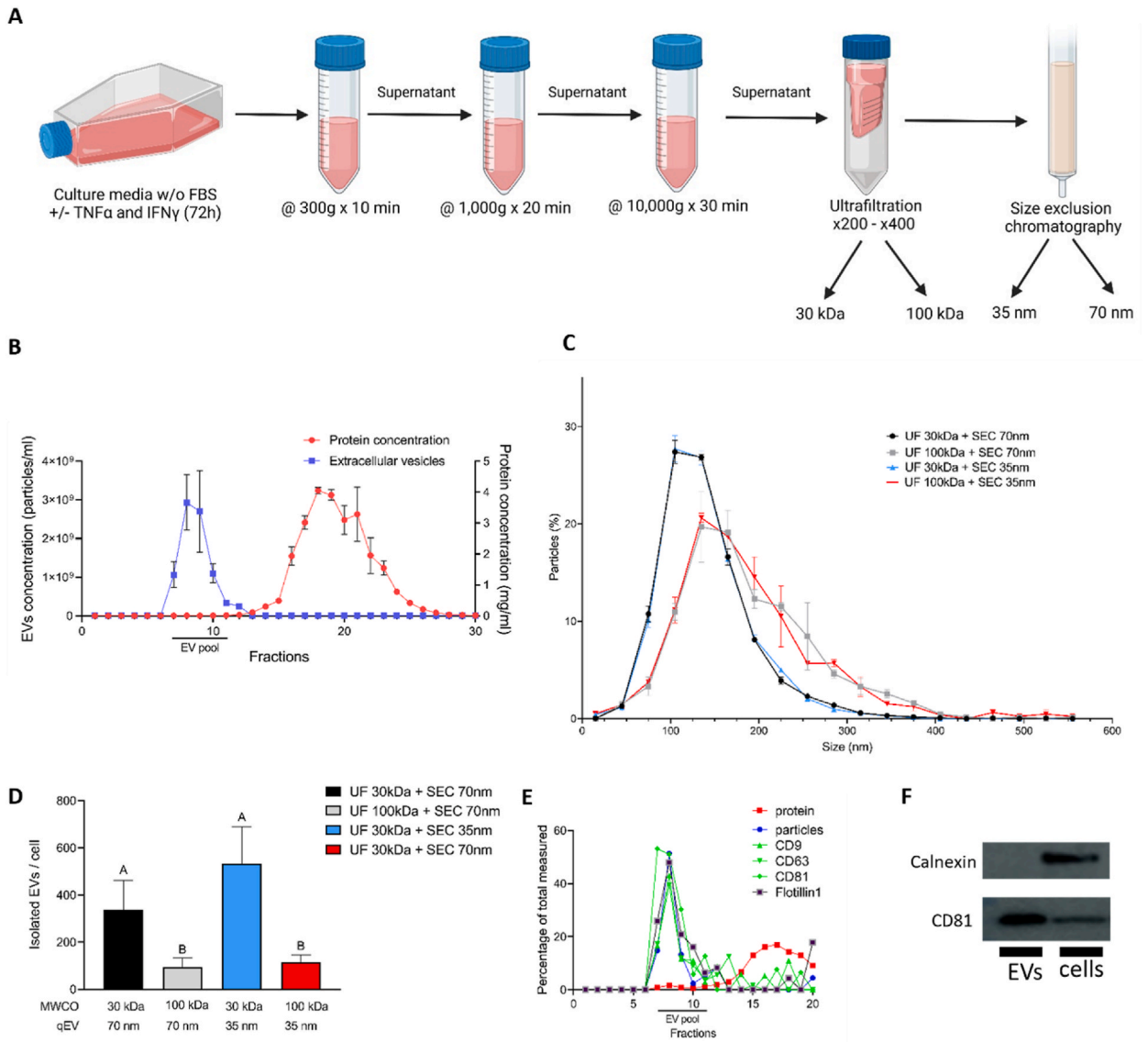


Fig. 1. Isolation and characterization of SCAP-EV. A. EV isolation workflow B. Quantification of protein (micro BCA) and number of EV (NTA) in each fraction after the SEC with a pore size of 35 nm (n = 3) C. Size distribution of isolated EV comparing 2 ultrafiltration cutoffs (30 and 100 kDa) and 2 size exclusion chromatography pore sizes (35 and 70 nm) (n = 3) D. Quantification of isolated EV per cell (n = 3) E. Delfia Immunoassay on EV positive markers (CD9, CD63, CD81 and Flotillin 1) F. Western Blot on a negative marker of EV (calnexin) and on a positive marker of EV (CD81) (full image in Supplementary data S1).

3.2. Identification of SCAP-EV miRNA content

As EV are thought to be one of the main miRNA transporters [28], we first analyzed the miRNA content of steady-state SCAP-EV. Around 100,000 mapped reads were detected from non-activated SCAP-EV, while 236 miRNA were identified (Supplementary data S2). The identified small RNAs were mainly miscellaneous small RNA, long non-coding RNA and small nuclear RNA (Fig. 2A). Among the miRNA contained in EV isolated from non-activated SCAP, 22 had a count higher than 1000 (Supplementary data S3). A miRNA-target prediction analysis revealed that 1868 genes are potential targets of these miRNA (Supplementary data S4). When a KEGG enrichment analysis was performed on the targeted genes, 36 pathways that could be impacted by the 22 miRNA were identified (Fig. 3). The 5 more affected pathways were MAPK signaling pathway, pathways in cancer, neurotrophin signaling pathway, regulation of actin cytoskeleton and focal adhesion pathways.

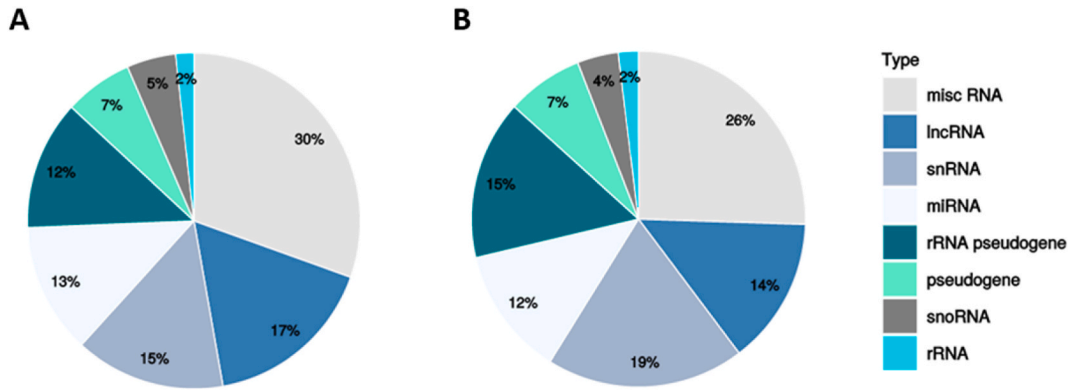


Fig. 2. Distribution of small RNAs identified in SCAP-EV. Content of RNA in A. non-activated SCAP-EV and B. in activated SCAP-EV. miscRNA: miscellaneous small RNA; lncRNA: long non-coding RNA; snRNA: small nuclear RNA; miRNA: microRNA; rRNA: ribosomal RNA; snoRNA: small nucleolar RNA.

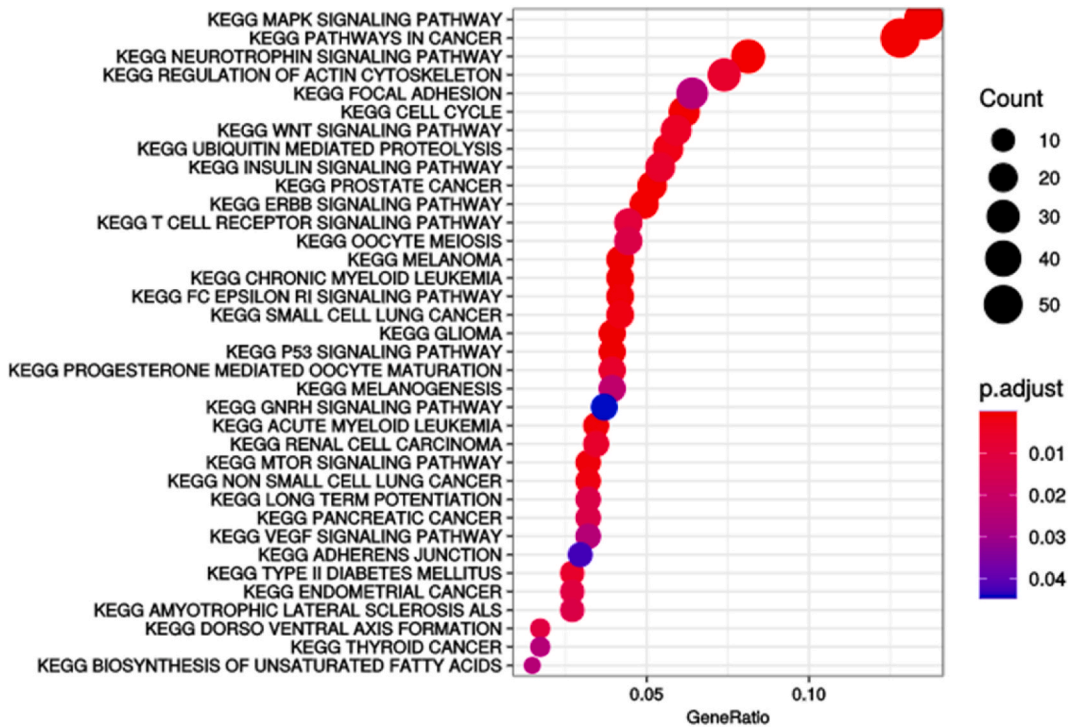


Fig. 3. KEGG pathway analysis of genes potentially targeted by the miRNA identified in EV from non-activated SCAP. KEGG analysis was performed on the 1868 potential targets of the 22 miRNA identified in EV with a count higher than 1000.

3.3. Impact of SCAP activation on EV composition

Then, to study how SCAP activation would impact their EV content, miRNA and lipid from EV produced by SCAP subjected to a pro-inflammatory stimulus (namely TNF α and IFN- γ) were analyzed and compared to EV produced from non-activated SCAP.

In terms of protein concentration, no differences were observed between non-activated SCAP-EV and activated SCAP-EV (2631 \pm 125 μ g/ml and 2483 \pm 237 μ g/ml for 10⁹ EV, respectively).

3.3.1. miRNA content

The proportion of the different small RNAs, including miRNA, was not impacted by the activation of SCAP (Fig. 2B). More precisely, 120,000 mapped reads were detected from activated SCAP-EV, while 248 miRNA were identified in activated SCAP-EV (Supplementary data S5).

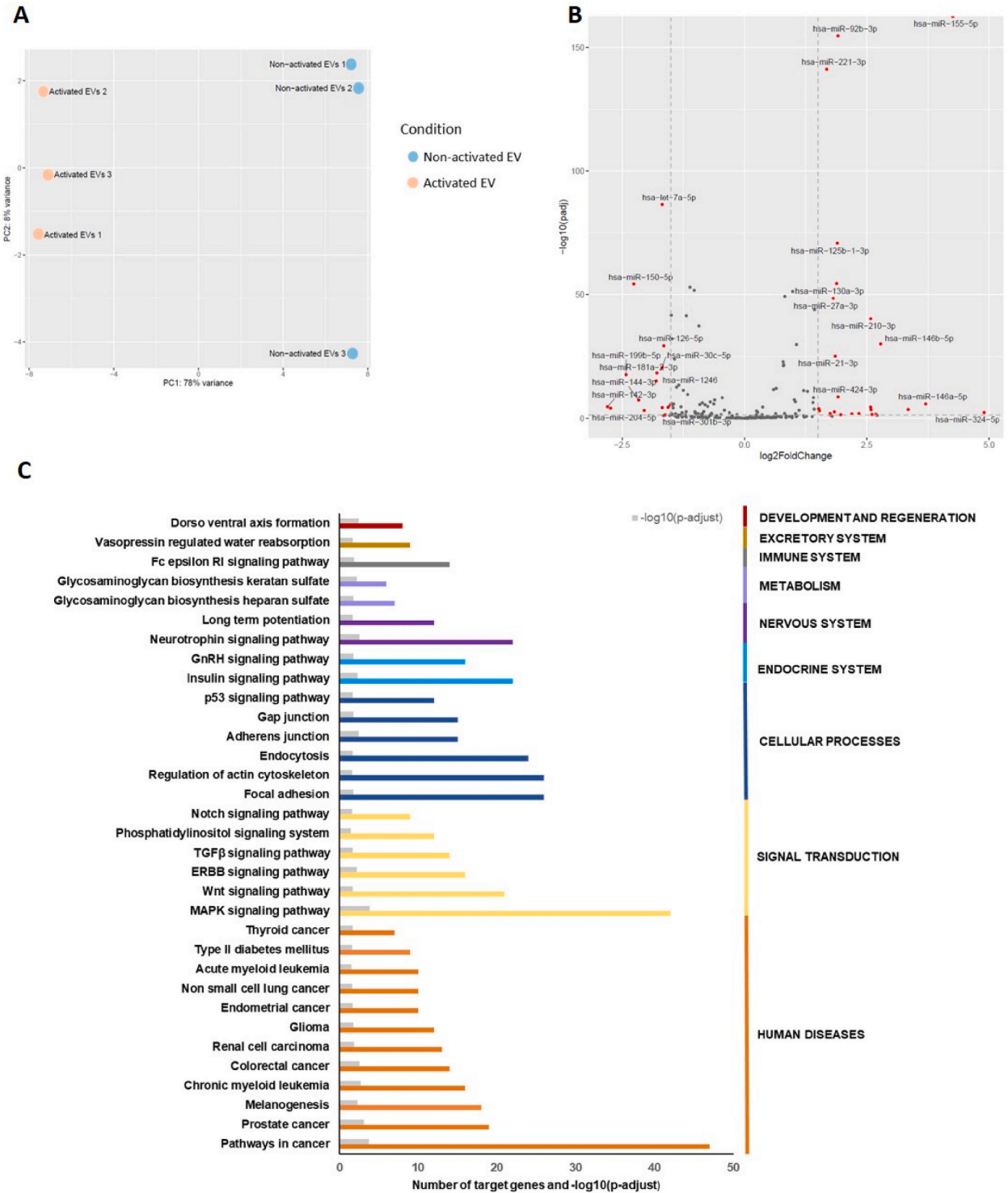


Fig. 4. Impact of SCAP activation on the miRNA content of EV. A. Principal component analysis. B. Volcano-plot of miRNA differentially expressed in EV isolated from activated SCAPs versus non-activated SCAPs. C. KEGG enrichment analysis of targeted genes of differentially expressed miRNA and the BRITE hierarchy. The color bars showed the number of target genes involved in the pathway while the grey bars represent the $-\log_{10}(p\text{-value})$. (For interpretation of the references to color in this figure legend, the reader is referred to the Web version of this article.)

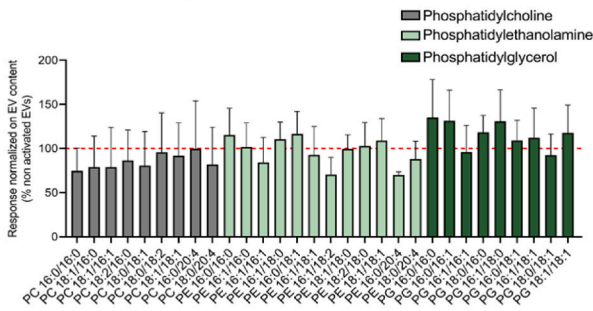
To evaluate the impact of pro-inflammatory cytokines on the miRNA content of SCAP-EV, a differential expression analysis comparing non-activated and activated SCAP-EV miRNA was performed. Principal component analysis (PCA) showed a clear separation between non-activated and activated samples along PC1 (78% of variance), suggesting a significant effect of SCAP activation on the miRNA content of their EV (Fig. 4A). Among the differentially expressed miRNA, 25 and 15 were significantly up-regulated and down-regulated, respectively (Fig. 4B). More precisely, miR-155-5p, miR-324-5p, miR-92b-3p, miR-221-3p and miR-146a-5p were the most up-regulated in EV of activated SCAP, while let-7a-5p, miR-150-5p, miR-204-5p and miR-142-5p were the most down-regulated. A KEGG analysis was performed on the potential targets of these 40 miRNA (Supplementary data S6) that identified 33 pathways potentially affected by SCAP activation (Fig. 4C).

3.3.2. Lipid content

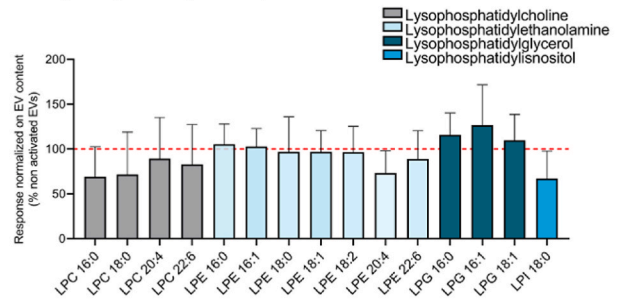
In order to study the impact of SCAP activation on their EV lipid content, the proportion of phospholipids, ceramides, sulfatides and sphingomyelin was compared between EV isolated from activated SCAP and non-activated SCAP. The lipidomic analysis allowed the identification of numerous lipids present in SCAP-EV (Fig. 5) but no significant difference in the lipid composition was observed between non-activated and activated SCAP-EV (Fig. 5A–E).

The impact of SCAP activation on EV content of lipid mediators like eicosanoids or their precursor was also assessed. In our experimental setting, only leukotriene B4, 11-hydroxyeicosatetraenoic acid, arachidonic acid and 2-arachidonoylglycerol (2-AG) were

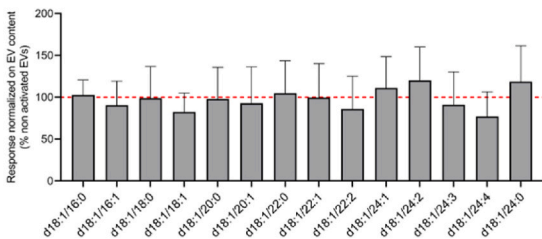
A. Phospholipids



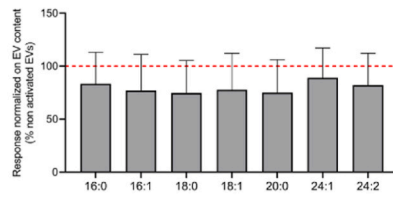
B. Lysophospholipids



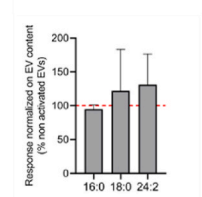
C. Ceramides



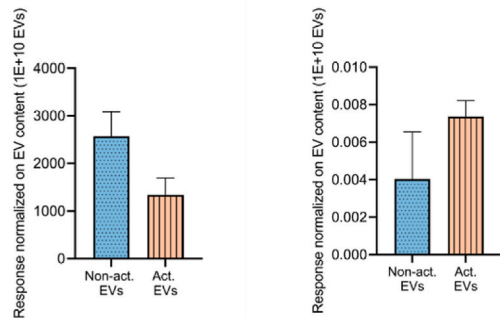
D. Sphingomyelin



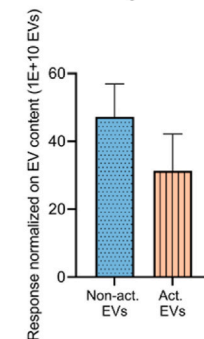
E. Sulfatides



F. Arachidonic acid G. 2-AG



H. LTB4



I. 11-HETE

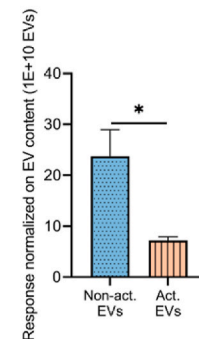


Fig. 5. Lipid content of non-activated SCAP-EV and activated SCAP-EV. A. Phospholipids B. Lysophospholipids C. Ceramides D. d18:1 Sphingomyelins E. d18:1 Sulfatides F. Arachidonic acid G. 2-Arachidonoylglycerol (2-AG) H. Leukotriene B₄ I. 11-HETE. The dotted red line represents the detection in non-activated SCAP-EV. (For interpretation of the references to color in this figure legend, the reader is referred to the Web version of this article.)

detected. While 2-AG tended to increase in activated SCAP-EV (Fig. 5F), while arachidonic acid (Fig. 5G) and leukotriene B₄ (Fig. 5H) tended to decrease, only 11-HETE was significantly decreased in activated SCAP-EV (Fig. 5I).

3.4. Impact of SCAP-EV on microglial pro-inflammatory cytokine expression

To assess whether SCAP-EV, non-activated and activated, would have an immunomodulatory effect, as observed for their parent cells [16], LPS-stimulated BV2 microglial cells were incubated with EV to study their impact on pro-inflammatory cytokine gene expression was studied.

First, EV were incubated with steady-state BV2 cells for 8 h and 24 h. Treating BV2 cells with SCAP-EV, isolated either from activated or non-activated cells, significantly reduced interleukin (IL)-1 β gene expression after 8 h of incubation but had no significant impact on the other tested cytokines (Fig. 6A). The EV from activated SCAP induced an increase of inducible nitric oxide synthase (iNOS) gene expression after 24 h of incubation (the same tendency was observed after 8 h) (Fig. 6B).

Then, the effect of SCAP-EV was assessed on LPS-activated BV2 cells. Our data show that, regardless of the incubation time, neither non-activated nor activated SCAP-EV were able to significantly impact the gene expression of pro-inflammatory cytokines of BV2 cells

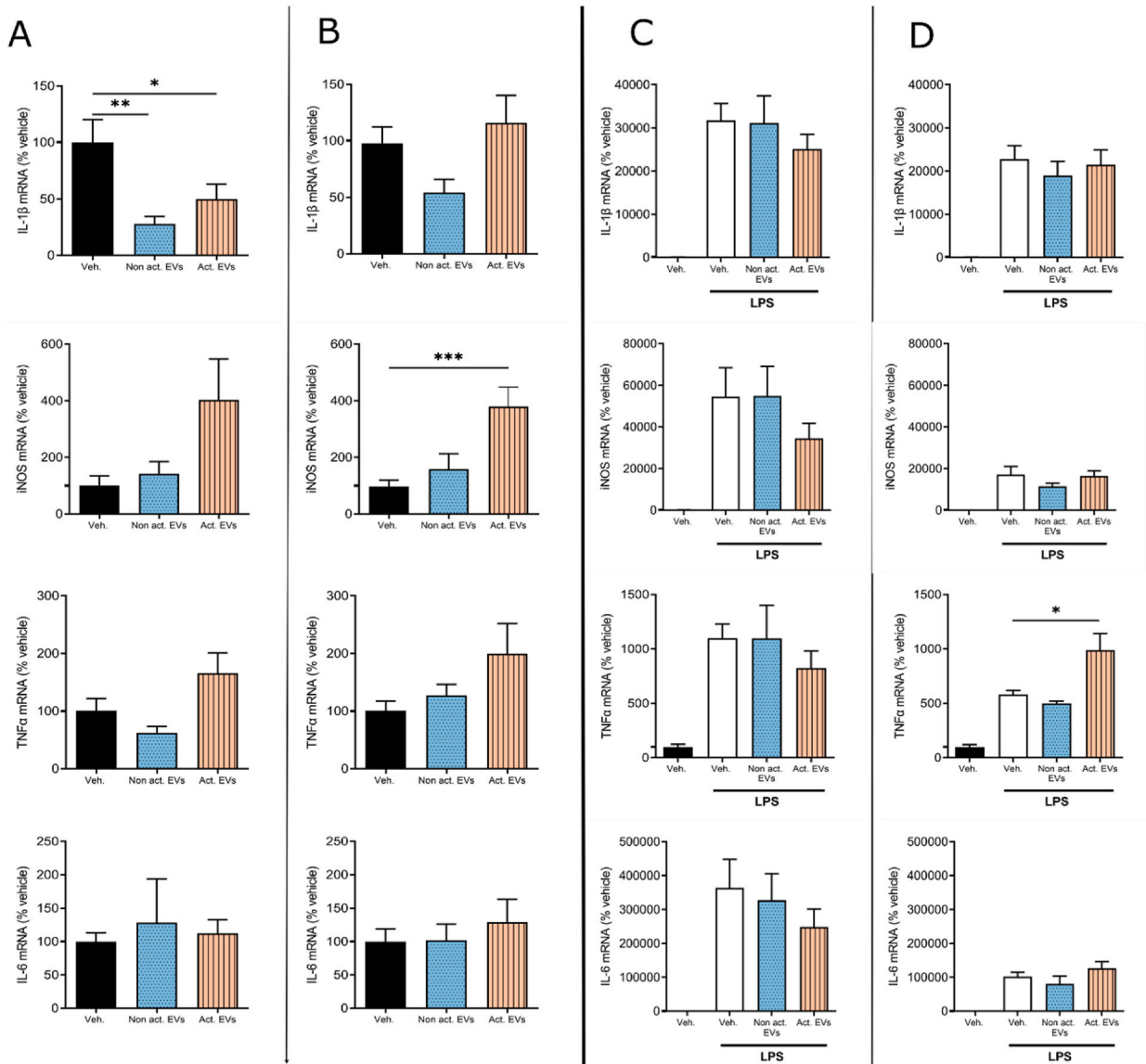


Fig. 6. Impact of SCAP-EV on the expression of pro-inflammatory cytokines by BV2 cells. Cells were treated with EV (5×10^9) isolated from non-activated or activated SCAP for 8 h (A) or 24 h (B). Alternatively, BV2 were activated by LPS (100 ng/ml) for 1 h and then treated with EV (5×10^9) isolated from non-activated or activated SCAP for 8 h (C) or 24 h (D). The black bars show the impact of vehicle (PBS) on non-activated BV2 cells while the white bars show the influence of vehicle (PBS) on LPS-activated BV2 cells. N = 3, n = 4. *p < 0.05, **p < 0.005, ***p < 0.001.

(Fig. 6C and D). Only TNF α was significantly affected by activated SCAP-EV after 24 h of incubation. After 8 h of incubation, activated SCAP-EV tended to reduce pro-inflammatory gene expression but it was not significant.

3.5. Impact of SCAP-EV on pro-inflammatory cytokine expression in spinal cord sections

To study the impact of non-activated and activated SCAP-EV on a more complex model of the central nervous system, the same experiment was conducted on mouse spinal cord sections. Spinal cord sections were activated by LPS and then incubated with EV for 8 h or 24 h. Activated SCAP-EV induced a decrease of iNOS gene expression after 8 h of incubation (Fig. 7A) but had no impact on the expression of cytokines. Non-activated and activated SCAP-EV were not able to significantly affect the expression of pro-inflammatory cytokines and iNOS after 24 h of incubation (Fig. 7B). TNF α and IL-6 secretion followed the same pattern (Supplementary data S7).

3.6. Impact of the protein fraction of activated SCAP conditioned medium on microglial pro-inflammatory cytokine expression

As it has been shown that the effect of contaminant proteins could be misattributed to the EV [29], we evaluated the impact of pooled protein fractions from activated-SCAP conditioned medium on LPS-activated BV2 cells. BV2 cells were pre-activated with LPS and incubated for 8 h with a pool of the protein fractions [12–30] or with EV from activated-SCAP. Of note, the protein pool was concentrated to the same fold than the EV.

Here, activated SCAP-EV significantly decreased the gene expression of IL-1 β , iNOS and IL-6 (Fig. 8) with the same fold than observed in Fig. 6, confirming the impact of activated SCAP-EV on BV2 cell pro-inflammatory marker expression. The highest fold decrease was observed with IL-6 and iNOS (fold decrease of 1.5, Supplementary data S8). However, no effect of the protein fractions was observed, except on IL-6 mRNA expression.

4. Discussion

The interest in EV, as biomarkers, therapeutic tool or drug delivery vehicles, has constantly increased during the last decade [8]. In our previous work, we showed that SCAP secreted immunomodulatory molecules in the presence of pro-inflammatory stimuli [16]. They also decreased the pro-inflammatory cytokine expression of LPS-activated BV2 cells when co-cultured with them [15]. Although EV from SCAP have previously been reported [28,29] for their effect on angiogenesis and on cisplatin-induced acute kidney injury, the objective of this work was to isolate EV based on their size and, for the first time, determine whether SCAP exposure to a pro-inflammatory stimulus would impact the composition of their EV and their effect on activated glial cells. Our hypothesis was that

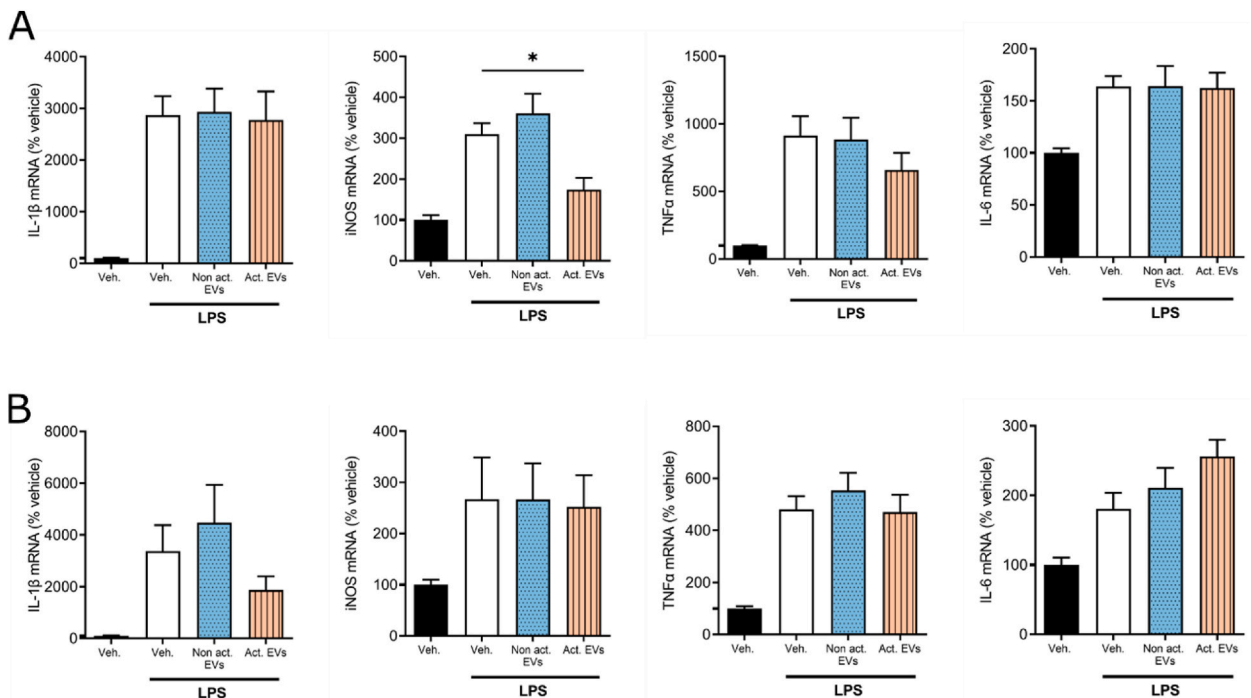


Fig. 7. Impact of SCAP-EV on the expression of pro-inflammatory cytokines by spinal cord sections. Mouse spinal cord sections were incubated with LPS (100 ng/ml) for 1 h before treatment with EV (5×10^9) isolated from non-activated or activated SCAP for 8 h (A) or 24 h (B). The black bars show the impact of vehicle (PBS) on non-activated spinal cord sections while the white bars show the influence of vehicle (PBS) on LPS-activated spinal cord sections. N = 3, n = 4. *p < 0.05.

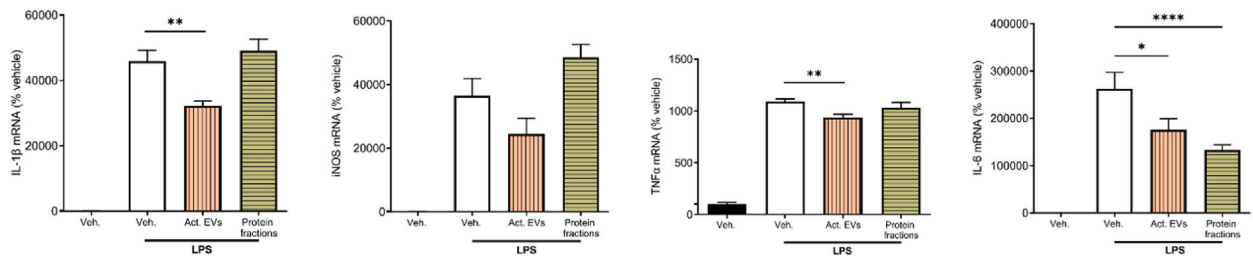


Fig. 8. Impact of activated SCAP-EV and their pooled protein fractions on the expression of pro-inflammatory cytokines by BV2 cells. BV2 cells were incubated with LPS (100 ng/ml) for 1 h and then treated for 8 h with EV (5×10^9) isolated from activated SCAP or a pool of their protein fractions. The black bars show the impact of vehicle (PBS) on non-activated BV2 cells while the white bars show the influence of vehicle (PBS) on LPS-activated BV2 cells. N = 3, n = 4. * $p < 0.05$, ** $p < 0.005$, *** $p < 0.0001$.

the reduction of neuroinflammation observed with SCAP could be due, at least partially, to the EV they secrete. For the first time, we demonstrated that it was possible to isolate EV from SCAP, with limited protein contaminants. Regarding the size and the positive markers of these particles, the term EV includes exosomes and small microvesicles. We then analyzed SCAP-EV small RNA and lipid content and showed that when SCAP were incubated with pro-inflammatory cytokines, the type but not the number of miRNA associated to EV was affected while SCAP activation did not have a strong impact on their lipid composition. Finally, when we compared the impact of SCAP-EV and of the protein fraction of SCAP conditioned medium on microglial pro-inflammatory markers, a reduction of their expression was observed that was independent of the protein present in the medium. Thus, due to their intrinsic properties, SCAP-EV seem to be an interesting cell-free nanotechnology.

A protocol was developed and optimized for the collection of EV from SCAP conditioned medium with the aim to ally the highest recovery and the highest purity possible. We were able to obtain EV, as assessed by the presence of positive markers and the absence of negative markers, and to separate EV quite efficiently from soluble proteins and apolipoproteins by combining ultrafiltration and SEC. This method is quite reproducible and has been recently successfully used in our laboratory to isolate EV from other sources. Several methods have been reported in the literature to isolate EV [30]. The specific selection of one method, or combination of methods, strongly depends on the subsequent use of the EV. While ultracentrifugation is probably the most straightforward and historically the most used, it tends to damage EV and to co-isolate soluble proteins with EV [30]. As for downstream characterization and functional testing these two parameters are important, we decided to combine ultrafiltration and SEC to isolate the EV from SCAP [31]. This combination is becoming more and more popular, but this is the first time, to our knowledge, where the cutoff and the pore size of the ultrafiltration membrane and SEC, respectively, were directly compared and combined to reach the best compromise between yield and purity. We obtained a suspension of EV with a very low concentration of proteins (5.6 pg/ 10^6 EV) that we hypothesized to be EV-associated proteins. This point is particularly important as therapeutic effects attributed to EV could be due, at least partially, to co-isolated soluble cytokines or growth factors and not due to EV themselves [29].

Among the different molecules carried by EV, miRNA is one of the most studied family as they are involved in the physiopathology of various diseases. As such, they have a high therapeutic potential [32]. Gao et al. showed for instance that bone marrow derived MSC-EV were able to transfer miR-21-5p to neurons and improve cognitive functions in a rat model of early brain injury [33]. The most abundant miRNA in non-activated SCAP-EV were miR-22-3p, miR-181a-5p, miR-100-5p and miR-127-5p which all seem to play a role in the regulation or suppression of the inflammatory response [34–37]. Moreover, Luo et al. showed that miR-100-5p was enriched in exosomes of stem cells from human exfoliated deciduous teeth and thus were able to reduce inflammation via its action on mTOR signaling pathway [36]. However, miRNA that are known to induce inflammation were also found in non-activated SCAP-EV such as miR-486-5p, miR-92a-3p and miR-222-3p [38–40]. Among the 22 most expressed miRNA in non-activated SCAP-EV, 13 miRNA were also found in Human Wharton's Jelly MSC-EV [41]. By targeting the Notch and MAPK/ERK signaling cascades, these miRNA were able to drive oligodendroglial maturation in the central nervous system.

As the SCAP secretome is influenced by cell exposure to pro-inflammatory cytokines [16], we hypothesized that their EV content might also be modulated in these conditions. We compared the miRNA content of non-activated SCAP-EV and activated SCAP-EV. MiR-155 and miR-146 were among the miRNA with the highest fold increase. This correlates with an increased expression of these two miRNA in immune cells after an exposure to TNF α and IFN- γ [42]. MiR-155 is known to inhibit the immune response mediated by SOCS1 in macrophages while miR-146 targets IRAK1, IRAK2 and TRAF6 which are both involved in innate response via Toll-like receptor and IL-1 receptor signaling [43,44]. However, these two miRNA seem also to have anti-inflammatory effect as miR-155 can be a link between adaptive and innate immunity [45]. Contradictory effects for the same miRNA have been then reported in the literature, mostly depending on the scientific question, the models used and the type of output. This highlights the limitations of the *in silico* prediction of miRNA biological effects. However additional studies are needed to identify miRNA targets and their physiological function [46]. The multiplicity of miRNA target genes also complicates the prediction of their biological impact. Thus, understanding the effect of multiple miRNA delivered by EV remains a challenge.

The KEGG pathway analysis highlighted 33 pathways potentially affected by SCAP activation. Among them, pathways in cancer, MAPK signaling pathway, focal adhesion, regulation of actin cytoskeleton and endocytosis pathways are the five most affected pathways. About 500 genes are involved in pathways in cancer and 21 pathways are connected to them. The presence of miRNAs involved in these pathways in SCAP-EV could highlight a potential role of EV in the mediation of some cancer processes, such as

metastasis [47]. MAPK signaling pathway is the second most affected pathway and is involved in multiple cellular processes including MSC proliferation and differentiation. As the ability of IFN- γ to increase the differentiation potential of MSC has been previously demonstrated, this could explain why this pathway is affected by SCAP activation with IFN- γ and TNF α [48]. Focal adhesion and regulation of actin cytoskeleton are two pathways involved in immunomodulatory processes. Indeed, regulation of actin cytoskeleton is a key mediator of communication between MSC and B cells while focal adhesion regulates cell migration, including migration of cells toward site of inflammation and homing [47]. TNF α is known to regulate MSC migration in order to lead the cells to the inflamed area. Thus, it is not surprising that these 2 pathways are also affected by the activation of SCAP with TNF α and IFN- γ . The fifth most affected pathway is endocytosis. It could be explained by its involvement in EV generation and a modification of EV production under stress conditions such as a pro-inflammatory environment [49].

As major components of EV envelop and as potent biological mediators, the focus on EV lipid composition increased recently, but only a few studies on the subject have yet been published [50,51]. When looking at the lipid content of human bone marrow MSC-EV, cells that can be considered of the same family than SCAP, Holopainen et al. detected ceramides, diacylglycerol, phospholipids, lysophospholipids and sphingomyelin [50]. We report for the first time the lipid composition of SCAP-EV that seems quite similar to the one reported by Holopainen et al. However, due to differences in report format, method of data analysis and standardization, it is difficult to establish quantitative comparisons with other works. Based on the same hypothesis than for the miRNA, we also evaluated whether the SCAP-EV lipid composition was affected by SCAP incubation with pro-inflammatory cytokines. In our setting we did not see a major impact on EV lipid composition. Only eicosanoid 11-HETE was significantly reduced after SCAP activation. Its role in inflammation has not been studied yet. To the extent of our knowledge, no other work has reported the impact of inflammation on EV lipid composition.

Finally, with the objective to decipher whether SCAP-EV would recapitulate SCAP anti-inflammatory effect on microglial cells and on spinal cord sections [15], SCAP-EV isolated from activated and non-activated SCAP were incubated with BV2 cells and mouse spinal cord sections, treated or not with LPS. EV decreased the gene expression of pro-inflammatory cytokines in LPS-treated macrophages by a 1.5-fold. Similar results were observed on spinal cord slices. Our results are consistent with other studies that reported an anti-inflammatory effect of about a 2 fold-decrease of pro-inflammatory cytokines for EV of different origins [52–54]. We also assessed the effect of the protein fraction isolated from activated SCAP conditioned medium after EV isolation. To minimize interpretation bias, attention was paid to concentrate the pooled protein fractions to a similar extent than the pooled EV fractions. The effect of activated SCAP-EV on pro-inflammatory cytokines expression by LPS-activated BV2 cells was similar to what we previously observed, with this time a significant reduction of the tested pro-inflammatory cytokine expression. The protein pool had no effect on LPS-activated BV2 cells, when looking at pro-inflammatory cytokine gene expression, with the exception of IL-6.

As we chose to isolate EV from SCAP under serum starvation (72 h) to limit FBS protein content and thus protein contamination of EV suspension, the properties of the SCAP producing the EV, and thus the EV, might be different from other protocols reported in the literature. This could have impacted EV content [55], and anti-inflammatory potential, and thus may explain the limited effects observed with SCAP-EV. In the future, replacing serum starvation by a synthetic serum-free medium might be an alternative worth considering. Other optimizations of EV production with other chemical signals such as Cytochalasin-B [56] or hypoxia [57] may also help to obtain better immunomodulatory effects.

It is also important to keep in mind that the effect of human MSC-EV could depend on the parent cells (type, source and culture conditions), the concentration of EV and the model used [22]. Thus, some articles reported a pro-inflammatory effect of MSC-EV. Kang et al. for example highlighted a role of EV from LPS-preconditioned periodontal ligament stem cells in M1 polarization of macrophages while previous studies reported a M2 polarization of macrophages after treatment with LPS-preconditioned human umbilical cord MSC. This highlighted the impact on the origin of MSC on the effect of their EV on macrophage polarization [58]. The multitude of different protocols and settings complicates the comparison between studies, especially given that what is considered negative results or lack of effect are unfortunately less reported in the literature.

5. Conclusion

Our aim was to fully characterize EV produced by SCAP and explore whether they would be affected by a pro-inflammatory stimulus. We also aimed to decipher if SCAP-EV would be responsible, at least partially, for the immunomodulation observed when SCAP are co-cultured with microglial cells or spinal cord. We thus optimized a protocol that allowed us to collect EV as free as possible from contaminants and we analyzed their miRNA content and lipid composition. We have shown that SCAP were able to respond to a pro-inflammatory stimulus by modifying the miRNA content of their EV but not their lipid composition. We observed a slight reduction of the gene expression of pro-inflammatory markers in a microglial cell line, albeit in the range of what was observed by some other studies. We thus conclude that the EV are likely not the key mediators in the reported effects of SCAP, at least in the model we used.

Data availability statement

The datasets generated during and/or analyzed during the current study are available from the corresponding author on reasonable request.

The dataset generated and analyzed during the current study is available in the GEO repository under the number GSE208577 at <https://www.ncbi.nlm.nih.gov/geo/query/acc.cgi?acc=GSE208577>.

CRediT authorship contribution statement

Viridiane Gratpain: Writing – review & editing, Writing – original draft, Methodology, Investigation, Conceptualization. **Axelle Lorient:** Writing – original draft, Formal analysis, Data curation. **Pauline Bottemanne:** Methodology, Formal analysis, Data curation. **Ludovic d’Auria:** Methodology, Investigation, Data curation. **Romano Terrasi:** Methodology, Investigation. **Valéry L. Payen:** Methodology, Investigation. **Vincent van Pesch:** Writing – review & editing, Resources, Funding acquisition. **Giulio G. Muccioli:** Writing – review & editing, Validation, Resources, Funding acquisition. **Anne des Rieux:** Writing – review & editing, Writing – original draft, Supervision, Resources, Project administration, Funding acquisition.

Declaration of competing interest

The authors declare that they have no known competing financial interests or personal relationships that could have appeared to influence the work reported in this paper.

Acknowledgements

Anne des Rieux is an Honorary FRS-FNRS Senior Research Associate. This work has been supported by the Fondation Charcot Stichting, the Communauté Française de Belgique in the scope of actions de recherche concertées (ARC) and the Université catholique de Louvain. Adrien Paquot (BPBL, LDRI, UCLouvain) is acknowledged for his skillful help with lipid analysis. The authors thank Prof. Anibal Diogenes for providing the human SCAP.

Appendix A. Supplementary data

Supplementary data to this article can be found online at <https://doi.org/10.1016/j.heliyon.2024.e27025>.

References

- [1] G. Raposo, W. Stoorvogel, Extracellular vesicles: exosomes, microvesicles, and friends, *J. Cell Biol.* 200 (4) (2013) 373–383.
- [2] G. van Niel, D.R.F. Carter, A. Clayton, D.W. Lambert, G. Raposo, P. Vader, Challenges and directions in studying cell-cell communication by extracellular vesicles, *Nat. Rev. Mol. Cell Biol.* 23 (5) (2022) 369–382.
- [3] S. Stremersch, S.C. De Smedt, K. Raemdonck, Therapeutic and diagnostic applications of extracellular vesicles, *J. Contr. Release* 244 (Pt B) (2016) 167–183.
- [4] F. Urabe, N. Kosaka, K. Ito, T. Kimura, S. Egawa, T. Ochiya, Extracellular vesicles as biomarkers and therapeutic targets for cancer, *Am. J. Physiol. Cell Physiol.* 318 (1) (2020) C29–C39.
- [5] R.E. Lane, D. Korbie, M.M. Hill, M. Trau, Extracellular vesicles as circulating cancer biomarkers: opportunities and challenges, *Clin. Transl. Med.* 7 (1) (2018) 14.
- [6] P.D. Robbins, A.E. Morelli, Regulation of immune responses by extracellular vesicles, *Nat. Rev. Immunol.* 14 (3) (2014) 195–208.
- [7] P. Vader, E.A. Mol, G. Pasterkamp, R.M. Schiffelers, Extracellular vesicles for drug delivery, *Adv. Drug Deliv. Rev.* 106 (Pt A) (2016) 148–156.
- [8] V. Gratpain, A. Mwema, Y. Labrak, G.G. Muccioli, V. van Pesch, A. des Rieux, Extracellular vesicles for the treatment of central nervous system diseases, *Adv. Drug Deliv. Rev.* 174 (2021) 535–552.
- [9] **Allogenic Mesenchymal Stem Cell Derived Exosome in Patients With Acute Ischemic Stroke** [Available from: <https://ClinicalTrials.gov/show/NCT03384433>].
- [10] I.K. Herrmann, M.J.A. Wood, G. Fuhrmann, Extracellular vesicles as a next-generation drug delivery platform, *Nat. Nanotechnol.* 16 (7) (2021) 748–759.
- [11] S. Staubach, F.N. Bauer, T. Tertel, V. Borger, O. Stambouli, D. Salzig, et al., Scaled preparation of extracellular vesicles from conditioned media, *Adv. Drug Deliv. Rev.* 177 (2021) 113940.
- [12] J.P. Armstrong, M.N. Holme, M.M. Stevens, Re-engineering extracellular vesicles as smart nanoscale therapeutics, *ACS Nano* 11 (1) (2017) 69–83.
- [13] M. Yanez-Mo, P.R. Siljander, Z. Andreu, A.B. Zavec, F.E. Borrás, E.I. Buzas, et al., Biological properties of extracellular vesicles and their physiological functions, *J. Extracell. Vesicles* 4 (2015) 27066.
- [14] N. Kim, S.G. Cho, Clinical applications of mesenchymal stem cells, *Korean J. Intern. Med. (Engl. Ed.)* 28 (4) (2013) 387–402.
- [15] P. De Berdt, P. Bottemanne, J. Bianco, M. Alhouayek, A. Diogenes, A. Lloyd, et al., Stem cells from human apical papilla decrease neuro-inflammation and stimulate oligodendrocyte progenitor differentiation via activin-A secretion, *Cell. Mol. Life Sci.* 75 (15) (2018) 2843–2856.
- [16] P. De Berdt, K. Vanvarenberg, B. Ucakar, C. Bouzin, A. Paquot, V. Gratpain, et al., The human dental apical papilla promotes spinal cord repair through a paracrine mechanism, *Cell. Mol. Life Sci.* 79 (5) (2022) 252.
- [17] M. Riazifar, M.R. Mohammadi, E.J. Pone, A. Yeri, C. Lasser, A.I. Segaliny, et al., Stem cell-derived exosomes as nanotherapeutics for autoimmune and neurodegenerative disorders, *ACS Nano* 13 (6) (2019) 6670–6688.
- [18] C. Thery, K.W. Witwer, E. Aikawa, M.J. Alcaraz, J.D. Anderson, R. Andriantsitohaina, et al., Minimal information for studies of extracellular vesicles 2018 (MISEV2018): a position statement of the International Society for Extracellular Vesicles and update of the MISEV2014 guidelines, *J. Extracell. Vesicles* 7 (1) (2018) 1535750.
- [19] N.B. Ruparel, J.F. de Almeida, M.A. Henry, A. Diogenes, Characterization of a stem cell of apical papilla cell line: effect of passage on cellular phenotype, *J. Endod.* 39 (3) (2013) 357–363.
- [20] M.R. Friedlander, S.D. Mackowiak, N. Li, W. Chen, N. Rajewsky, miRDeep2 accurately identifies known and hundreds of novel microRNA genes in seven animal clades, *Nucleic Acids Res.* 40 (1) (2012) 37–52.
- [21] M.I. Love, W. Huber, S. Anders, Moderated estimation of fold change and dispersion for RNA-seq data with DESeq2, *Genome Biol.* 15 (12) (2014) 550.
- [22] Y. Ru, K.J. Kechris, B. Tabakoff, P. Hoffman, R.A. Radcliffe, R. Bowler, et al., The multiMiR R package and database: integration of microRNA-target interactions along with their disease and drug associations, *Nucleic Acids Res.* 42 (17) (2014) e133.
- [23] T. Wu, E. Hu, S. Xu, M. Chen, P. Guo, Z. Dai, et al., clusterProfiler 4.0: a universal enrichment tool for interpreting omics data, *Innovation (N Y)*. 2 (3) (2021) 100141.
- [24] V. Mutemberezi, B. Buisseret, J. Masquelier, O. Guillemot-Legrès, M. Alhouayek, G.G. Muccioli, Oxysterol levels and metabolism in the course of neuroinflammation: insights from in vitro and in vivo models, *J. Neuroinflammation* 15 (1) (2018) 74.

- [25] Y. Labrak, B. Heurtaut, B. Frisch, P. Saulnier, E. Lepeltier, V.E. Miron, et al., Impact of anti-PDGFRalpha antibody surface functionalization on LNC uptake by oligodendrocyte progenitor cells, *Int. J. Pharm.* 618 (2022) 121623.
- [26] A. Mwema, P. Bottemanne, A. Paquot, B. Ucakar, K. Vanvarenberg, M. Alhouayek, et al., Lipid nanocapsules for the nose-to-brain delivery of the anti-inflammatory bioactive lipid PGD(2)-G, *Nanomedicine* 48 (2023) 102633.
- [27] M. Alhouayek, D.M. Lambert, N.M. Delzenne, P.D. Cani, G.G. Muccioli, Increasing endogenous 2-arachidonoylglycerol levels counteracts colitis and related systemic inflammation, *Faseb. J.* 25 (8) (2011) 2711–2721.
- [28] M. Ktach, C. Thery, Communication by extracellular vesicles: where we are and where we need to go, *Cell* 164 (6) (2016) 1226–1232.
- [29] T.E. Whitaker, A. Nagelkerke, V. Nele, U. Kauscher, M.M. Stevens, Experimental artefacts can lead to misattribution of bioactivity from soluble mesenchymal stem cell paracrine factors to extracellular vesicles, *J. Extracell. Vesicles* 9 (1) (2020) 1807674.
- [30] C. Gardiner, D. Di Vizio, S. Sahoo, C. Thery, K.W. Witwer, M. Wauben, et al., Techniques used for the isolation and characterization of extracellular vesicles: results of a worldwide survey, *J. Extracell. Vesicles* 5 (2016) 32945.
- [31] B.J. Benedikter, F.G. Bouwman, T. Vajen, A.C.A. Heinzmann, G. Grauls, E.C. Mariman, et al., Ultrafiltration combined with size exclusion chromatography efficiently isolates extracellular vesicles from cell culture media for compositional and functional studies, *Sci. Rep.* 7 (1) (2017) 15297.
- [32] M. Nakano, M. Fujimiya, Potential effects of mesenchymal stem cell derived extracellular vesicles and exosomal miRNAs in neurological disorders, *Neural. Regen. Res.* 16 (12) (2021) 2359–2366.
- [33] X. Gao, Y. Xiong, Q. Li, M. Han, D. Shan, G. Yang, et al., Extracellular vesicle-mediated transfer of miR-21-5p from mesenchymal stromal cells to neurons alleviates early brain injury to improve cognitive function via the PTEN/Akt pathway after subarachnoid hemorrhage, *Cell Death Dis.* 11 (5) (2020) 363.
- [34] X. Wang, Y. Wang, M. Kong, J. Yang, MiR-22-3p suppresses sepsis-induced acute kidney injury by targeting PTEN, *Biosci. Rep.* 40 (6) (2020).
- [35] Y. Cui, K. Yin, Y. Gong, Y. Qu, H. Liu, H. Lin, Atrazine induces necroptosis by miR-181-5p targeting inflammation and glycometabolism in carp lymphocytes, *Fish Shellfish Immunol.* 94 (2019) 730–738.
- [36] P. Luo, C. Jiang, P. Ji, M. Wang, J. Xu, Exosomes of stem cells from human exfoliated deciduous teeth as an anti-inflammatory agent in temporomandibular joint chondrocytes via miR-100-5p/mTOR, *Stem Cell Res. Ther.* 10 (1) (2019) 216.
- [37] T. Xie, J. Liang, N. Liu, Q. Wang, Y. Li, P.W. Noble, et al., MicroRNA-127 inhibits lung inflammation by targeting IgG Fc gamma receptor I, *J. Immunol.* 188 (5) (2012) 2437–2444.
- [38] Q. Luo, J. Zhu, Q. Zhang, J. Xie, C. Yi, T. Li, MicroRNA-486-5p promotes acute lung injury via inducing inflammation and apoptosis by targeting OTUD7B, *Inflammation* 43 (3) (2020) 975–984.
- [39] L. Casadei, F. Calore, C.J. Creighton, M. Guescini, K. Batte, O.H. Iwenofu, et al., Exosome-derived miR-25-3p and miR-92a-3p stimulate liposarcoma progression, *Cancer Res.* 77 (14) (2017) 3846–3856.
- [40] Y. Zhang, J. Yang, X. Zhou, N. Wang, Z. Li, Y. Zhou, et al., Knockdown of miR-222 inhibits inflammation and the apoptosis of LPS-stimulated human intervertebral disc nucleus pulposus cells, *Int. J. Mol. Med.* 44 (4) (2019) 1357–1365.
- [41] M.S. Joerges-Messerli, G. Thomi, V. Haesler, I. Keller, P. Renz, D.V. Surbek, et al., Human wharton's jelly mesenchymal stromal cell-derived small extracellular vesicles drive oligodendroglial maturation by restraining MAPK/ERK and Notch signaling pathways, *Front. Cell Dev. Biol.* 9 (2021) 622539.
- [42] D. Baltimore, M.P. Boldin, R.M. O'Connell, D.S. Rao, K.D. Taganov, MicroRNAs: new regulators of immune cell development and function, *Nat. Immunol.* 9 (8) (2008) 839–845.
- [43] J. Ye, R. Guo, Y. Shi, F. Qi, C. Guo, L. Yang, miR-155 regulated inflammation response by the SOCS1-STAT3-PCDC4 Axis in atherogenesis, *Mediat. Inflamm.* 2016 (2016) 8060182.
- [44] C. Zhou, L. Zhao, K. Wang, Q. Qi, M. Wang, L. Yang, et al., MicroRNA-146a inhibits NF-kappaB activation and pro-inflammatory cytokine production by regulating IRAK1 expression in THP-1 cells, *Exp. Ther. Med.* 18 (4) (2019) 3078–3084.
- [45] A. Rodriguez, E. Vigorito, S. Clare, M.V. Warren, P. Couttet, D.R. Soond, et al., Requirement of bic/microRNA-155 for normal immune function, *Science* 316 (5824) (2007) 608–611.
- [46] S. Mockly, H. Seitz, Inconsistencies and limitations of current microRNA target identification methods, *Methods Mol. Biol.* 1970 (2019) 291–314.
- [47] A. Adamo, J. Brandi, S. Caligola, P. Delfino, R. Bazzoni, R. Carusone, et al., Extracellular vesicles mediate mesenchymal stromal cell-dependent regulation of B cell PI3K-akt signaling pathway and actin cytoskeleton, *Front. Immunol.* 10 (2019) 446.
- [48] X. He, W. Jiang, Z. Luo, T. Qu, Z. Wang, N. Liu, et al., IFN-gamma regulates human dental pulp stem cells behavior via NF-kappaB and MAPK signaling, *Sci. Rep.* 7 (2017) 40681.
- [49] G. van Niel, G. D'Angelo, G. Raposo, Shedding light on the cell biology of extracellular vesicles, *Nat. Rev. Mol. Cell Biol.* 19 (4) (2018) 213–228.
- [50] M. Holopainen, R.A. Colas, S. Valkonen, F. Tigistu-Sahle, K. Hyvarinen, F. Mazzacava, et al., Polyunsaturated fatty acids modify the extracellular vesicle membranes and increase the production of proresolving lipid mediators of human mesenchymal stromal cells, *Biochim. Biophys. Acta Mol. Cell Biol. Lipids* 1864 (10) (2019) 1350–1362.
- [51] R.C. Lai, S.S. Tan, R.W. Yeo, A.B. Choo, A.T. Reiner, Y. Su, et al., MSC secretes at least 3 EV types each with a unique permutation of membrane lipid, protein and RNA, *J. Extracell. Vesicles* 5 (2016) 29828.
- [52] N. Pacienza, R.H. Lee, E.H. Bae, D.K. Kim, Q. Liu, D.J. Prockop, et al., In vitro macrophage assay predicts the in vivo anti-inflammatory potential of exosomes from human mesenchymal stromal cells, *Mol. Ther. Methods Clin. Dev.* 13 (2019) 67–76.
- [53] L.A. Vonk, S.F.J. van Dooremalen, N. Liv, J. Klumperman, P.J. Coffey, D.B.F. Saris, et al., Mesenchymal stromal/stem cell-derived extracellular vesicles promote human cartilage regeneration in vitro, *Theranostics* 8 (4) (2018) 906–920.
- [54] P. Xu, Y. Xin, Z. Zhang, X. Zou, K. Xue, H. Zhang, et al., Extracellular vesicles from adipose-derived stem cells ameliorate ultraviolet B-induced skin photoaging by attenuating reactive oxygen species production and inflammation, *Stem Cell Res. Ther.* 11 (1) (2020) 264.
- [55] K.W. Witwer, E.I. Buzas, L.T. Bemis, A. Bora, C. Lasser, J. Lotvall, et al., Standardization of sample collection, isolation and analysis methods in extracellular vesicle research, *J. Extracell. Vesicles* 2 (2013).
- [56] M.O. Gomzikova, A.M. Aimaltdinov, O.V. Bondar, I.G. Starostina, N.V. Gorshkova, O.A. Neustroeva, et al., Immunosuppressive properties of cytochalasin B-induced membrane vesicles of mesenchymal stem cells: comparing with extracellular vesicles derived from mesenchymal stem cells, *Sci. Rep.* 10 (1) (2020) 10740.
- [57] C. Lo Sicco, D. Reverberi, C. Balbi, V. Ulivi, E. Principi, L. Pascucci, et al., Mesenchymal stem cell-derived extracellular vesicles as mediators of anti-inflammatory effects: endorsement of macrophage polarization, *Stem Cells Transl. Med.* 6 (3) (2017) 1018–1028.
- [58] H. Kang, M.J. Lee, S.J. Park, M.S. Lee, Lipopolysaccharide-preconditioned periodontal ligament stem cells induce M1 polarization of macrophages through extracellular vesicles, *Int. J. Mol. Sci.* 19 (12) (2018).